September 2006

Fundamental and biotechnological applications of neutron scattering measurements for macromolecular dynamics

M. Tehei
University of Wollongong, moeava@uow.edu.au

R. Daniel
University of Waikato, New Zealand

G. Zaccai
Institut Laue-Langevin, Grenoble, France

Fundamental and biotechnological applications of neutron scattering measurements for macromolecular dynamics

Abstract

To explore macromolecular dynamics on the picosecond timescale, we used neutron spectroscopy. First, molecular dynamics were analyzed for the hyperthermophile malate dehydrogenase from Methanococcus jannaschii and a mesophilic homologue, the lactate dehydrogenase from Oryctolagus cunniculus muscle. Hyperthermophiles have elaborate molecular mechanisms of adaptation to extremely high temperature. Using a novel elastic neutron scattering approach that provides independent measurements of the global flexibility and of the structural resilience (rigidity), we have demonstrated that macromolecular dynamics represents one of these molecular mechanisms of thermoadaptation. The flexibilities were found to be similar for both enzymes at their optimal activity temperature and the resilience is higher for the hyperthermophilic protein. Secondly, macromolecular motions were examined in a native and immobilized dihydrofolate reductase (DHFR) from Escherichia coli. The immobilized mesophilic enzyme has increased stability and decreased activity, so that its properties are changed to resemble those of the thermophilic enzyme. Are these changes reflected in dynamical behavior? For this study, we performed quasielastic neutron scattering measurements to probe the protein motions. The residence time is 7.95 ps for the native DHFR and 20.36 ps for the immobilized DHFR. The average height of the potential barrier to local motions is therefore increased in the immobilized DHFR, with a difference in activation energy equal to 0.54 kcal/mol, which is, using the theoretical rate equation, of the same order than expected from calculation.

Keywords

Neutron scattering, Dynamics, Biotechnology, Extreme temperature, Immobilization, DHFR

Disciplines

Life Sciences | Physical Sciences and Mathematics | Social and Behavioral Sciences

Publication Details

This article was originally published as Tehei, M, Daniel, R, & Zaccai, G, Fundamental and biotechnological applications of neutron scattering measurements for macromolecular dynamics, European Biophysics Journal 35(7), 2006, 551-558. Original article is available here.

Eur Biophys J
DOI 10.1007/s00249-006-0082-6

REVIEW

Fundamental and biotechnological applications of neutron scattering measurements for macromolecular dynamics

Moeava Tehei · Roy Daniel · Giuseppe Zaccai

Received: 26 January 2006 / Revised: 17 June 2006 / Accepted: 26 June 2006

Abstract To explore macromolecular dynamics on the picosecond timescale, we used neutron spectroscopy. First, molecular dynamics were analyzed for the hyperthermophile malate dehydrogenase from *Methanococcus jannaschii* and a mesophilic homologue, the lactate dehydrogenase from *Oryctolagus cunniculus* muscle. Hyperthermophiles have elaborate molecular mechanisms of adaptation to extremely high temperature. Using a novel elastic neutron scattering approach that provides independent measurements of the global flexibility and of the structural resilience (rigidity), we have demonstrated that macromolecular dynamics represents one of these molecular mechanisms of thermoadaptation. The flexibilities were found to be similar for both enzymes at their optimal activity temperature and the resilience is higher for the hyperthermophilic protein. Secondly, macromolecular motions were examined in a native and immobilized dihydrofolate reductase (DHFR) from *Escherichia coli*. The immobilized mesophilic enzyme has increased stability and decreased activity, so that its properties are changed to resemble those of the thermophilic enzyme. Are these changes reflected in dynamical behavior? For this study, we performed quasielastic neutron scattering measurements to probe the protein motions. The residence time is 7.95 ps for the native DHFR and 20.36 ps for the immobilized DHFR. The average height of the potential barrier to local motions is therefore increased in the immobilized DHFR, with a difference in activation energy equal to 0.54 kcal/mol, which is, using the theoretical rate equation, of the same order than expected from calculation.

M. Tehei (✉)
CNR-INFM, c/o Institut Laue-Langevin,
6 rue Jules Horowitz, BP 156,
38042 Grenoble Cedex 9, France
e-mail: v-tehei@ill.fr

R. Daniel
Department of Biological Sciences,
University of Waikato, Private Bag 3105,
Hamilton, New Zealand

G. Zaccai
Institut Laue-Langevin, 6 rue Jules Horowitz,
BP 156, 38042 Grenoble Cedex 9, France

G. Zaccai
Institut de Biologie Structurale,
UMR 5075 CEA-CNRS-UJF,
41 rue Jules Horowitz, 38027 Grenoble, France

Introduction

Dynamics on the picosecond to nanosecond timescale allow macromolecules to achieve the stability and fluctuations, and, therefore, the necessary rigidity and flexibility to perform their biological functions (Lehnert et al. 1998; Tehei et al. 2001, 2005). Neutron spectroscopy is particularly adapted to the study of these motions, because neutron wavelengths ($\approx$ Å) and energies ($\approx$ meV) match, respectively, the amplitudes and frequencies of molecular motions (Gabel et al. 2002; Smith 1991).

This mini review focuses on two areas of research. Firstly, the enzyme malate dehydrogenase from the hyperthermophile Archaeon *Methanococcus jannaschii* (*Mj* MalDH) (Tehei et al. 2005). This extremophile,

like all organisms living in extreme environments (extremophiles) has to develop molecular mechanisms of adaptation to one or several more extreme physico-chemical conditions. Using neutron spectroscopy, we have demonstrated that macromolecular dynamics presents one of these molecular mechanisms of adaptation. We present results for *Mj* MalDH and a mesophilic homologue, lactate dehydrogenase from *Oryctolagus cunniculus* muscle (*Oc* LDH). Thermo-adaptation appears to have been achieved by evolution through selection of appropriate resilience, in order to preserve specific macromolecule structure, while allowing the conformational flexibility required for activity.

Secondly, the immobilized *Escherichia coli* (*E. coli)* dihydrofolate reductase (DHFR) (Tehei et al. 2006) is an essential enzyme required for normal folate metabolism in prokaryotes and eukaryotes, and it is recognized as a drug target for inhibiting DNA synthesis in rapidly proliferating cells such as cancer cells (Huennekens 1994). The comparative study of the native and the immobilized DHFR showed that the average height of the potential barrier of the enzyme to achieve the local motions necessary for its activity is increased in the immobilized DHFR, which may increase the activation energy for the enzyme catalysis, decreasing the observed rate. These results suggest that the local motions on the picosecond timescale may act as a lubricant for those associated with DHFR activity occurring on slower millisecond timescale. Experiments indicate a significantly slower catalytic reaction rate for the immobilized *E. coli* DHFR. However, the immobilization of the DHFR is on the exterior of the enzyme and essentially distal to the active site, thus this phenomenon has broad implications for the action of drugs distal to the active site.

Experimental

The hyperthermophile malate dehydrogenase from *Methanococcus jannaschii* (*Mj* MalDH)

Malate dehydrogenase from the hyperthermophile archaeon *Methanococcus jannaschii* is a member of the LDH-like family of malate dehydrogenases, which are tetrameric and have similar structures to the LDH (Lee et al. 2001; Madern 2000, 2002). *Mj* MalDH was compared to its mesophilic homologue, the lactate dehydrogenase from *Oryctolagus cunniculus* muscle (*Oc* LDH).

The instantaneous activities of the enzymes were measured as a function of temperature. The temperatures of optimal activity are 37°C for *Oc* LDH and 90°C for *Mj* MalDH. The relative stabilities of the enzymes were assessed by residual activity measurements and circular dichroism using guanidinium hydrochloride as denaturant. The residual activity is abolished in *Oc* LDH after incubation at about 50°C and in *Mj* MalDH after incubation above 90°C. The guanidinium chloride unfolding transition concentrations for *Oc* LDH and *Mj* MalDH are 1.3 and 2.1 M, respectively. Taken together, these data show that the hyperthermophilic protein is significantly more stable with a temperature of optimal activity higher (Tehei et al. 2005).

Immobilized dihydrofolate reductase

Dihydrofolate reductase catalyzes the NADPH-dependent reduction of 7,8-dihydrofolate to 5,6,7,8-tetrahydrofolate (THF). Many compounds of pharmacological value, such as methotrexate and trimethoprim work by inhibition of DHFR. DHFR is also recognized as a drug target for inhibiting DNA synthesis in rapidly proliferating cells such as cancer cells (Huennekens 1994).

The use of enzyme immobilization has expanded greatly in the last decade due to its potential applications in several fields including as biocatalysts, bioreactors, biosensors and in clinical use (Blun and Coulet 1990; Klibanov 1983; Tanaka et al. 1993). Immobilization can offer several advantages, such as high concentration, the possibility of reuse, and separation of the biocatalyst from the reaction products (Katchalski-Katzir 1993; Klibanov 1983). One of the main advantage concerning immobilized enzymes is enhanced stability (Eggers and Valentine 2001; Simpson et al. 1991; Zhou and Dill 2001).

DHFR from *E. coli* was immobilized by covalently binding to Sunsphere H122 (Asahi Glass Co., Ltd., Yurakucho, Japan), according to an adaptation of the trichlorotriazine (TCT) methodology (Moreno and Sinisterra 1994; Sinisterra 1997). In this immobilization methodology, the activated groups of the support react with the enzyme through the amino group of lysine (Moreno and Sinisterra 1994). According to the nucleotide sequence, characterization and three-dimensional structure, there are six lysine residues located on the outer surface of the DHFR molecule and they have no role in the active site. The amount of immobilized enzyme was found to be 25 mg DHFR per 100 mg support, which is one of the highest ever observed. Using the TCT methodology to immobilize the lipase from Candida cylindracea to several supports, Moreno and Sinisterra (1994) (Moreno and

Sinisterra 1994) obtained loadings of between 2.7 and 12 mg per 100 mg of support. The immobilization of the DHFR through external lysine residues reduced the activity rate by a factor of about 7 and increased its stability (Tehei et al. 2006). It can be seen that whereas for the native DHFR the apparent optimum temperature for activity is 55°C, for the immobilized DHFR the apparent optimum has been raised to 70°C (Fig. 1). The immobilized mesophilic enzyme has increased stability and decreased activity, so that its properties are changed to resemble those of the thermophilic enzyme. How are these changes reflected in the dynamic behavior of the enzyme?

Macromolecular dynamics

Elastic incoherent neutron scattering, mean square fluctuation and resilience

Elastic experiments on the malate/lactate dehydrogenase samples described in this review were performed on the backscattering spectrometer IN13 at the Institute Laue Langevin, Grenoble, France (information on the Institute and the instrument is available on the web at: http://www.ill.fr). The instrument allows one to examine atomic motions in the space and time window of about 1 Å in 0.1 ns. All motions outside the window, such as the diffusion of bulk water (≈ 10 Å in 0.1 ns), hydration water mobility at the surface of a protein (Bellissent-Funel et al. 1996), small peptides or the smaller membrane components, e.g., do not contribute to the scattering signal, so that experiments could be performed in H_2O solvent (we recall that many of the previous neutron scattering experiments were performed in heavy water). In this space-time window and according to the Gaussian approximation, the incoherent elastic scattered intensity can be analyzed as (Smith 1991):

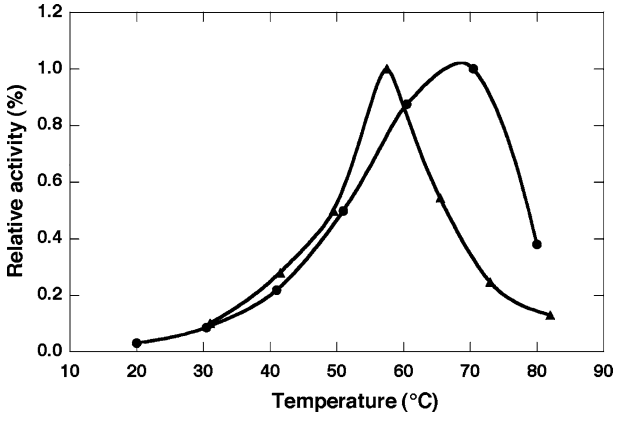

Fig. 1 Apparent optimum temperature for activity of native (*triangles*) and immobilized (*circles*) dihydrofolate reductase from *E. coli*

$$I(\mathbf{Q}, \mathbf{0} \pm \Delta\omega) = \mathbf{constant}.\exp\{(\mathbf{1/6})(-\langle \mathbf{u^2} \rangle \mathbf{Q^2})\}, \quad (1)$$

where $\mathbf{Q}$ is $4\pi \sin\theta/\lambda$, 2θ is the scattering angle and λ the incident neutron wavelength, $\langle u^2 \rangle$ values include all contributions to motions in the accessible space and time windows, from vibrational fluctuations (usually expressed as a Debye–Waller factor) as well as from diffusional motions. The validity of the Gaussian approximation for the mean square fluctuation $\langle u^2 \rangle$ and its analogy to the Guinier formalism for small angle scattering by particles in solution has been discussed by Réat et al. (1997) and more recently by Gabel (2005). In the Guinier formalism, the radius of gyration R_g^2 of a particle in solution is calculated (Guinier and Fournet 1955). The particle equivalent is the volume swept out by a single proton during the timescale of the experiment (~ 100 ps). The analogy holds if the motion is localized well within the space-time window defined by the $\mathbf{Q}$ and energy transfer ranges, respectively. The Guinier approximation is valid if $\sqrt{R_g^2 * \mathbf{Q^2}} \approx 1$. Following our definition of $\langle u^2 \rangle$, $R_g^2 = 1/2 * \langle u^2 \rangle$. As a consequence, the Gaussian approximation is valid in the domain where $\sqrt{\langle u^2 \rangle * \mathbf{Q^2}} \approx \sqrt{2}$. The mean square fluctuations $\langle u^2 \rangle$ at a given temperature T were calculated according to the Gaussian approximation as (Fig. 2):

$$\mathrm{Ln}[I(\mathbf{Q}, \mathbf{0} \pm \Delta\omega)] = \mathbf{constant} + \mathbf{A} * \mathbf{Q^2}. \quad (2)$$

The mean square fluctuations were therefore calculated as:

$$\langle u^2 \rangle = -6A. \quad (3)$$

Elastic incoherent scattering data were collected in a scattering vector range of 1.2 $\text{Å}^{-1} \leq \mathbf{Q} \leq 2.2$ Å^{-1}. The $\langle u^2 \rangle$ values were then plotted as a function of absolute temperature T (Fig. 3). The value of the root mean square fluctuation $\sqrt{\langle u^2 \rangle}$ in absolute Å units, quantifies the global flexibility of the system studied. An effective mean force constant $\langle k' \rangle$, defining mean resilience (rigidity), can be calculated from the derivative of $\langle u^2 \rangle$ plotted versus temperature, T (Bicout and Zaccai 2001; Zaccai 2000) (Fig. 3):

$$\langle k' \rangle = 0.00276/(\mathrm{d}\langle u^2 \rangle/\mathrm{d}T). \quad (4)$$

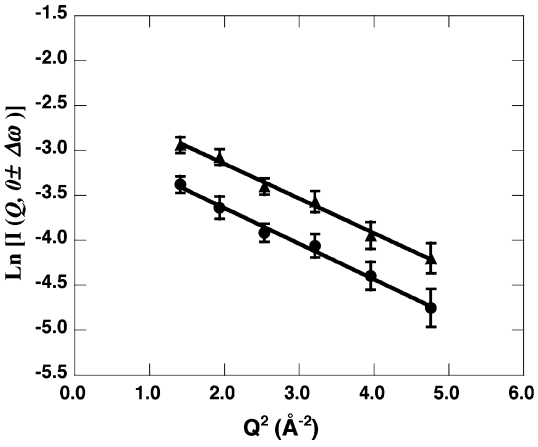

Fig. 2 Variation of Ln [I (**Q**, 0 ± $\Delta\omega$)] as a function of $\mathbf{Q}^2$ for the *Mj* MalDH at 279 K (*triangles*) and 310 K (*circles*), from which mean square fluctuations $\langle u^2 \rangle$ were calculated by using (2) and (3) (Tehei et al. 2005). The range of the fit corresponds to $1.5 \leq \sqrt{\langle u^2 \rangle}\mathbf{Q} \leq 3.1$. Beyond the **Q**-range illustrated, the Ln [I (**Q**, 0 ± $\Delta\omega$)] versus $\mathbf{Q}^2$ deviates from the straight line. The Guinier approximation is generally valid for the scattering curve of a particle of any shape, provided $\mathbf{Q}R_g$ is about 1. However, this approximation may remain valid to $\mathbf{Q}R_g$ beyond 1 depending on the shape of the particle. For ellipsoids of axial ratios about 1:1:1.7, the approximation is good significantly beyond $\mathbf{Q}R_g$ value of 1. For more compact shapes (e.g., the sphere, which is the most compact shape), the scattering curve deviates below the Guinier approximation, while for more asymmetric shapes (such as prolate or oblate ellipsoids with axial ratios 1:1: > 1.7 or 1:1: < 0.6, respectively, the scattering curve deviates above the Guinier approximation. Therefore, following our definition of $\langle u^2 \rangle$ and the asymmetric shape of the motions, the Gaussian approximation remains valid in the domain where $\sqrt{\langle u^2 \rangle}\mathbf{Q}$ is significantly beyond the value of $\sqrt{2}$

The numerical constants are chosen to express $\langle k' \rangle$ in Newton/meter (N/m) when $\langle u^2 \rangle$ is in Å^2 and T in Kelvin.

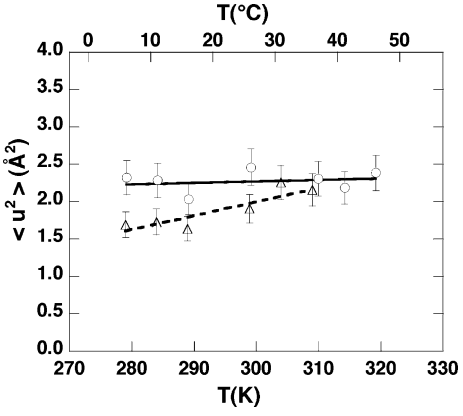

Fig. 3 Mean square fluctuation, $\langle u^2 \rangle$, versus temperature, T, measured on IN13 for *Oc* LDH (*triangles*) and *Mj* MalDH (*circles*). Effective mean force constants $\langle k' \rangle$, defining mean resilience (rigidity), was calculated from the slopes of the straight-line fits using (4) (Tehei et al. 2005)

Quasielastic incoherent neutron scattering, time of residence and activation energy

The experiments on DHFR samples were performed on the IN6 time of flight (TOF) spectrometer at the ILL (Institute Laue Langevin), Grenoble, using an incident wavelength of 5.12 Å, with an elastic energy resolution of 100 μeV (FWHM). The scattering was measured over a wave-vector range of $0.3 < \mathbf{Q} < 2.0$ Å^{-1} at 285 K.

It is usual to simplify the interpretation of data by separating the different kinds of contributions to motion according to their timescales and amplitudes, and subsequently making the hypothesis that these contributions are essentially not coupled between each other. Thus, vibrational motions occurring in the 10-fs timescale in a protein may safely be considered as independent from diffusive-type motions, which may occur in the picosecond–nanosecond timescale. This differentiation leads to the separation of a spectrum at a given **Q** between inelastic scattering, quasielastic scattering, and elastic scattering. In mathematical terms, the independence between the two types of motions, vibrational and diffusive, leads to a total scattering function expressed as the convolution of the respective scattering functions $S_{\text{tot}}(\mathbf{Q}, \omega) = [S_{\text{vib}}(\mathbf{Q}, \omega) \otimes S_{\text{diff}}(\mathbf{Q}, \omega)]$. In the quasielastic region of our spectra (i.e., $|\Delta E| \leq 0.6$–1.5 meV), the influence of the convolution with the high frequency vibrational spectral lines is essentially contained in the Debye–Waller factor, $\text{DW} = \text{e}^{-\langle u^2 \rangle \mathbf{Q}^2}$, which is simply a scaling factor that does not modify the shape of the quasielastic scattering function (Bée 1988). Hence,

$$S_{\text{q.e.theor}}(\mathbf{Q}, \omega) = \text{e}^{-\langle u^2 \rangle \mathbf{Q}^2} [S_{\text{diff}}(\mathbf{Q}, \omega)], \tag{5}$$

where $S_{\text{diff}}(\mathbf{Q}, \omega)$ arises from the picosecond timescale diffusive motions in the absence of vibrational modes and $\langle u^2 \rangle$ stands for the mean square displacement of high frequency vibration.

In the quasielastic incoherent approximation, the theoretical scattering function can be described by Bée (1988):

$$S_{\text{q.e.theor}}(\mathbf{Q}, \omega) = \text{e}^{-\langle u^2 \rangle \mathbf{Q}^2} \times \left[\left(A_0(\mathbf{Q}) \delta(\omega) + \sum_{i=1}^{n} A_i(\mathbf{Q}) L_{\text{internal}}(\Gamma_i, \omega) \right) \otimes L_{\text{D}}(\mathbf{Q}, \omega) \right], \tag{6}$$

where the expression within the square brackets describes the scattering function $S_{\text{diff}}(\mathbf{Q}, \omega)$. The internal motion in the protein is described by the expression within the brackets and $L_D(\mathbf{Q}, \omega)$ describes

an approximation to both global translational and rotational diffusion of the protein as a whole unit. $A_0(\mathbf{Q})$ is the elastic incoherent structure factor (EISF) and its $\mathbf{Q}$ dependence provide information about the geometry of the motion.

The quasielastic component $\sum_{i=1}^{n} A_i(\mathbf{Q}) L_{\text{internal}}(\Gamma_i, \omega)$, is a sum of Lorentzian functions:

$$L_{\text{internal}}(\Gamma_i, \omega) = \frac{1}{\pi} \frac{\Gamma_i(\mathbf{Q})}{\Gamma_i(\mathbf{Q})^2 + \omega^2}, \tag{7}$$

where Γ_i is the half-width at half-maximum of a Lorentzian peak.

Incoherent quasielastic neutron scattering, in the experimental conditions used, mainly measures motions on the picosecond timescales. In principle, global motions are much slower as than protein internal picosecond dynamics. In the immobilized sample, proteins are globally confined, and what is measured from quasielastic neutron scattering is a direct consequence of their internal picosecond motions. In the free DHFR solution, the expected apparent global diffusion constant, D, can be estimated as follows. For DHFR at infinite dilution in H_2O, $D = 1.1\ 10^{-6}\ \text{cm}^2/\text{s}$ (Baccanari et al. 1975). Because of the difference in viscosity between H_2O and D_2O, $\eta_{20°C}(D_2O)/\eta_{20°C}(H_2O) = 1.4$, D in D_2O is estimated to be $7.8 \times 10^{-7}\ \text{cm}^2/\text{s}$. Furthermore, at high protein concentration, D decreases exponentially with increasing protein concentration, and at the protein solution concentration used for the neutron scattering experiment (about 330 mg/ml), D is expected to be tenfold less than that at infinite dilution (Longeville et al. 2003; Riveros-Moreno and Wittenberg 1972). Thus, the diffusion coefficient of our protein solution in D_2O is expected to be $\sim 7.8 \times 10^{-8}\ \text{cm}^2/\text{s}$, i.e., $0.52\ \mu\text{eV}\ \text{Å}^2$. As a consequence, the quasielastic neutron energy transfers due to whole molecule protein motions in the present protein solution are much narrower than the instrumental energy resolution ($\approx 100\ \mu\text{eV}$) used in our measurements, and their contributions to the broadening the quasielastic scattering spectra can be assumed to be small and can thus be ignored. Equation (6) can then be reduced to:

$$S_{\text{q.e.theor}}(\mathbf{Q}, \omega) = \mathrm{e}^{-\langle u^2 \rangle \mathbf{Q}^2} \left[A_0(\mathbf{Q}) \delta(\omega) + \sum_{i=1}^{n} A_i(\mathbf{Q}) L_{\text{internal}}(\Gamma_i, \omega) \right]. \tag{8}$$

The theoretical scattering function (8) was fitted to the data with the standard ILL fitting program 'Profit' by using the following relation (information on the Institute and programs is available on the web at http://www.ill.fr):

$$S_{\text{meas}}(\mathbf{Q}, \omega) = \mathrm{e}^{-\hbar\omega/2k_B T} \left[s_{\text{q.e.theor}}(\mathbf{Q}, \omega) \otimes S_{\text{res}}(\mathbf{Q}, \omega) \right] + B_0, \tag{9}$$

in which a convolution with the spectrometer resolution function $S_{\text{res}}(\mathbf{Q}, \omega)$ and a detailed balance factor $\mathrm{e}^{-\hbar\omega/2k_B T}$ are applied. B_0 is the inelastic background due to the vibrational modes of lowest energy (the "lattice phonons") (Bée 1988). The fits were performed over the energy transfer range – 0.6 to + 1.5 meV. The $S_{\text{meas}}(\mathbf{Q}, \omega)$ of both the immobilized and free DHFR were found to be reasonably well fitted with a single Lorentzian function (Fig. 4).

Results and discussion

Intrinsic dynamics: comparison of the hyperthermophile *Mj* MalDH and a mesophilic homologue *Oc* LDH

Activity and stability data combined with neutron results for hyperthermophilic and mesophilic enzymes of the malate lactate dehydrogenase family, established a strong adaptation of root mean square fluctuation (global flexibility) and resilience (rigidity) to physiological temperature. The value of the global flexibility (1.5 Å) observed for *Oc* LDH and for *Mj* MalDH at their respective temperature of optimal activity (37°C for the mesophile and 90°C for the hyperthermophile) is essentially identical. The observation suggests that the enzymes have conformational flexibility adjusted to the optimum working temperature, in accordance with the hypothesis that adaptation of proteins to different physiological temperatures tends to maintain enzymes in 'corresponding states', characterized by similar conformational flexibility (Jaenicke 1991). The stability data show that the hyperthermophilic protein is significantly more stable with a temperature of optimal activity higher (Tehei et al. 2005). The mean resilience (rigidity) is an order of magnitude larger for *Mj* MalDH (1.50 N/m) than for *Oc* LDH (0.15 N/m). The higher stability of *Mj* MalDH is, therefore, correlated with higher resilience. By performing comparative analysis using the three-dimensional crystal structures and the sequences, we suggested mechanisms that govern the high thermal stability of *Mj* MalDH, through increased resilience. The structural bases of thermophilic stability in the (LDH-like)

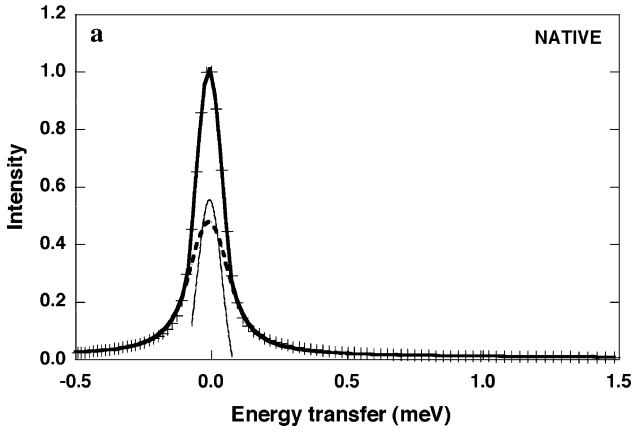

Fig. 4 Quasielastic spectrum of native (**a**) and immobilized (**b**) dihydrofolate reductase from *E. coli* at $T = 285$ K and $\mathbf{Q} = 1.73$ Å^{-1}. *Plus sign* indicates data and solid line is fitted curve using (9). The fit of the quasielastic spectra was performed for $-0.6 < \hbar\omega < 1.5$ meV. The different components correspond to the elastic peak (*dashed line*) and the Lorentzian line (*dotted line*) (Tehei et al. 2006)

malate dehydrogenase group have been discussed (Dalhus et al. 2002; Irimia et al. 2004). Enhanced stability arises from a combination of different mechanisms. This study indicates that several factors, such as increased the average charged (lysine, aspartate, arginine and glutamate) minus noncharged polar (asparagine, glutamine, serine and threonine) amino-acid percentage (Ch-Pol) value of protein sequence, increased of packing density as well as a reduction of number and total volume of internal cavities, increased of ion pairs and increased hydrogen bond interactions are responsible for a more stable protein and contribute to an observed increase in protein resilience suggesting the dominance of enthalpic contributions to the free energy landscape in the thermo-adaptation. For proteins in which entropic effects are dominant, a less resilient macromolecule will be more thermo-stable (Tehei et al. 2005). Thermoadaptation appears to have been achieved by evolution through selection of appropriate structural rigidity, in order to preserve specific protein structure, while allowing the conformational flexibility required for activity.

Biotechnological application: comparison of the immobilized and native dihydrofolate reductase

The $\langle u^2 \rangle$ values are 0.23 ± 0.04 and 0.19 ± 0.02 Å^2 for the native and the immobilized DHFR, respectively. The amplitude is slightly smaller for the immobilized DHFR but they are similar within error. The entropy change due to high frequency vibrational motions, which occurred on the femtosecond–picosecond timescale, is determined by $\Delta S_{\mathrm{vm}} = k_{\mathrm{B}} T * \mathrm{Ln}\left(\langle u^2 \rangle_{\mathrm{immobilizedDHFR}} / \langle u^2 \rangle_{\mathrm{nativeDHFR}}\right)$. The similar $\langle u^2 \rangle$ values of the native and the immobilized DHFR suggest that the high frequency vibrational motions do not contribute significantly to entropy changes in protein immobilization.

For picosecond timescale dynamics, the half-width at half-maximum, Γ of the Lorentzian in (7) is given as a function of $\mathbf{Q}^2$ in Fig. 5. Γ versus $\mathbf{Q}^2$ curves at first does not give zero intercepts in the low $\mathbf{Q}^2$ region for either immobilized or native DHFR. Then, the Γ values of the immobilized and native DHFR increase with $\mathbf{Q}^2$ and asymptotically approaches a constant value Γ_∞ at large $\mathbf{Q}$. The first feature indicates that the observed behavior is not free diffusion, but it is a typical characteristic of diffusion in a confined space (Bée 1988) and is approximately accounted for by the model of the model of Volino and Dianoux (1980), where a particle diffuse in sphere of radius *r*. The EISF

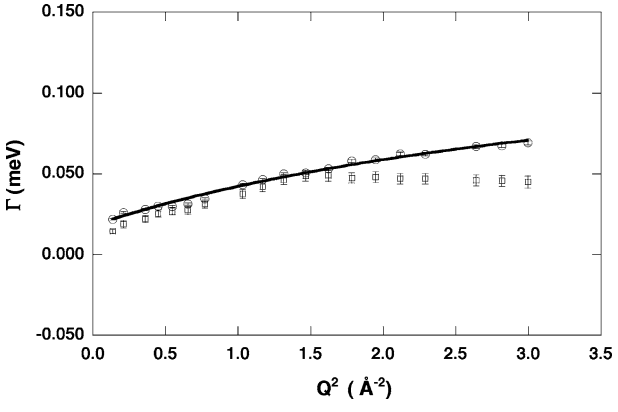

Fig. 5 Half-widths of the quasielastic Lorentzian function Γ as a function of $\mathbf{Q}^2$ for the immobilized (*squares*) and the native (*circles*) dihydrofolate reductase from *E. coli* at $T = 285$ K. The line results from the fit of Γ($\mathbf{Q}$) using (10) (Tehei et al. 2006)

and the radii of spheres values of the native and the immobilized DHFR are similar to within experimental error. Following Volino and Dianoux (1980), the diffusion coefficient D of the mobile protons diffusing within the sphere of radius r can be estimated from Γ_0, the limit of Γ at $\mathbf{Q} = 0$, with $\Gamma_0 = 4.333*D/r^2$. The internal diffusion coefficients D are also comparable for the native and the immobilized DHFR. These observations reinforce the theoretical quasielastic incoherent approximation we used in this work, where the contribution of the global diffusion of the protein as a whole unit is ignored (8). Furthermore, these observations also suggest that the contribution of internal diffusive motions is not significant for the activity changes of *E. coli* DHFR in our system.

At larger $\mathbf{Q}$ values, the line widths follows the well-known jump diffusion behavior, given by (Chen 1991; Egelstaff 1972):

$$\Gamma(\mathbf{Q}) = \frac{D\mathbf{Q}^2}{1 + D\mathbf{Q}^2\tau}. \tag{10}$$

In the high $\mathbf{Q}$ region, one observes motion on short length scales. On such scales, local jump motion of the protons becomes dominant. The residence time of a hydrogen atom on one site between jumps is $\tau = 1/\Gamma_\infty$, where Γ_∞ is obtained from the asymptotic behavior at high $\mathbf{Q}$, where Γ approaches a constant value. The Γ value at high $\mathbf{Q}$ of the native DHFR is still increasing, over the $\mathbf{Q}$-range examined, and has not yet reached the constant value. Therefore, this constant value was estimated by curve fitting using (10) and extrapolation to higher $\mathbf{Q}$ (Fig. 5). In contrast, the constant value Γ_∞ for the immobilized DHFR is reached over the $\mathbf{Q}$-range accessed. Therefore, this constant value is directly used to calculate the residence time. The result is residence time are $\tau = 7.95 \pm 1.02$ and 20.36 ± 1.80 ps for the native and immobilized DHFR, respectively. Using this model, our data imply that τ is larger for the immobilized DHFR. The local jump motion is related to the local potential energy barrier imposed on a proton by its environment. The height of this potential barrier is related to the residence time by the Arrhenius relation:

$$\tau = \tau_0 e^{(E_a/k_B T)}. \tag{11}$$

In (11), τ_0 is a pre exponential factor and E_a is the activation energy. Assuming that τ_0 is the same for the native and the immobilized DHFR, the activation energy difference between the two systems $\Delta E_a = k_B T[\ln(\tau_{\text{for immobilized DHFR}}) - \ln(\tau_{\text{for native DHFR}})]$ is 0.54 ± 0.12 kcal/mol.

In the picosecond timescale dynamics, neutron scattering results reveal the dependency of the length scale. The form of the results obtained is consistent with the restricted jump diffusion model (Hall and Ross 1981). Clearly, the Γ of the restricted jump diffusion model exhibits the characters both of the diffusion within a restricted volume (here a sphere) model and the jump diffusion model tending to asymptotic values at low and high $\mathbf{Q}$. At low $\mathbf{Q}$, we are mainly concerned with longer length scale, i.e., with the effects of the boundaries, which force the Γ to deviate from the $D\mathbf{Q}^2$ law (the Γ at low $\mathbf{Q}$ does not give zero intercepts) and to tend to a finite value, Γ_0. When the effect of confinement becomes less apparent, e.g., at room temperature, the Γ at low $\mathbf{Q}$ shows a finite Γ_0 without the plateau as it has been seen also in the Γ of others proteins solutions (Bu et al. 2000). Conversely, at large $\mathbf{Q}$, the nature of the local jump motions over shorter length scale predominate and, because the elementary displacements of the particles are not infinitely small, the Γ of the quasielastic component tends to the asymptotic value $1/\tau$.

According to the Arrhenius relation, the theoretical rate may be written as $k = k_B T/h \exp(-E_a/RT)$, where E_a is the activation energy barrier for the catalyzed reaction, k_B, the Boltzmann constant, h, the Planck constant, R, the gas constant and, T, the absolute temperature. Using this theoretical rate equation, we can calculate that the activation energy difference required to reduce the rate by a factor of 7 between the native and the immobilized DHFR is 1.10 kcal/mol. The observed activation energy difference between the immobilized and the native DHFR was 0.54 kcal/mol, which is of the same order but less than expected from calculation. This result indicates that the decrease in the rate for the immobilized DHFR may be due to an increase in the energy barrier. The rate of DHFR catalysis is expected to be influenced more by motions occurring on the millisecond timescale (Agarwal et al. 2002). Thus, this result suggests that local motions occurring on the picosecond timescale may have an influence on the much slower millisecond timescale of the catalytic activity. The results presented here show that although the immobilization of the DHFR is on the exterior of the enzyme and essentially distal to the active site, experiments indicate a significant decreasing of catalytic reaction rate. It is possible that the binding of ligands generally may exert a similar effect. In any event, this phenomenon has broad implications for protein engineering, drug design and effect of pharmacaphores distal to the active site.

Acknowledgments M.T. was supported by the Région Rhône-Alpes, France, the Marsden Fund of the Royal Society of New Zealand, New Zealand, and by the Istituto Nazionale Fisica della

Materia, Italy. We acknowledge supports from the EU under the DLAB contracts HPRI-CT-2001-50035 and RII3-CT-2003-505925, and the CNRS GEOMEX programme. We thank the CRG-IN13 and the Institut Laue Langevin for support and for providing the neutron facilities used for this work.

References

Agarwal PK, Billeter SR, Rajagopalan PT, Benkovic SJ, Hammes-Schiffer S (2002) Network of coupled promoting motions in enzyme catalysis. Proc Natl Acad Sci USA 99:2794–2799

Baccanari D, Phillips A, Smith S, Sinski D, Burchall J (1975) Purification and properties of *Escherichia coli* dihydrofolate reductase. Biochemistry 14:5267–5273

Bée M (1988) Quasielastic neutron scattering: principles and applications in solid state chemistry, biology and materials science. Adam Hilger, Bristol

Bellissent-Funel M-C, Zanotti J-M, Chen S-H (1996) Slow dynamics of water molecules on the surface of a globular protein. Faraday Discuss 103:281–294

Bicout DJ, Zaccai G (2001) Protein flexibility from the dynamical transition: a force constant analysis. Biophys J 80:1115–1123

Blun LJ, Coulet PR (1990) Biosensors: principles and applications. Dekker, New York

Bu Z, Neumann DA, Lee SH, Brown CM, Engelman DM, Han CC (2000) A view of dynamics changes in the molten globule-native folding step by quasielastic neutron scattering. J Mol Biol 301:525–536

Chen SH (1991) Hydrogen bonded liquids. In: Dore JC, Teixeira J (eds) NATO ASI Series, vol 329. Kluwer, Dordrecht

Dalhus B, Saarinen M, Sauer UH, Eklund P, Johansson K, Karlsson A, Ramaswamy S, Bjork A, Synstad B, Naterstad K, Sirevag R, Eklund H (2002) Structural basis for thermophilic protein stability: structures of thermophilic and mesophilic malate dehydrogenases. J Mol Biol 318:707–721

Egelstaff PA (1972) Quasielastic neutron scattering for the investigation of diffusive motions in solids and liquids. Springer, Berlin Heidelberg, New York

Eggers DK, Valentine JS (2001) Molecular confinement influences protein structure and enhances thermal protein stability. Protein Sci 10:250–261

Gabel F (2005) Protein dynamics in solution and powder measured by incoherent elastic neutron scattering: the influence of Q-range and energy resolution. Eur Biophys J 34:1–12

Gabel F, Bicout D, Lehnert U, Tehei M, Weik M, Zaccai G (2002) Protein dynamics studied by neutron scattering. Q Rev Biophys 35:327–367

Guinier A, Fournet G (1955) Small angle scattering of X-rays. Wiley, New York

Hall PL, Ross DK (1981) Incoherent neutron scattering functions for random jump diffusion in bounded and infinite media. Mol Phys 42:673–682

Huennekens FM (1994) The methotrexate story: a paradigm for development of cancer chemotherapeutic agents. Adv Enzyme Regul 34:397–419

Irimia A, Vellieux FM, Madern D, Zaccai G, Karshikoff A, Tibbelin G, Ladenstein R, Lien T, Birkeland NK (2004) The 2.9A resolution crystal structure of malate dehydrogenase from Archaeoglobus fulgidus: mechanisms of oligomerisation and thermal stabilisation. J Mol Biol 335:343–356

Jaenicke R (1991) Protein stability and molecular adaptation to extreme conditions. Eur J Biochem 202:715–728

Katchalski-Katzir E (1993) Immobilized enzymes—learning from past successes and failures. Trends Biotechnol 11:471–478

Klibanov AM (1983) Immobilized enzymes and cells as practical catalysts. Science 219:722–727

Lee BI, Chang C, Cho SJ, Eom SH, Kim KK, Yu YG, Suh SW (2001) Crystal structure of the MJ0490 gene product of the hyperthermophilic archaebacterium *Methanococcus jannaschii*, a novel member of the lactate/malate family of dehydrogenases. J Mol Biol 307:1351–1362

Lehnert U, Reat V, Weik M, Zaccai G, Pfister C (1998) Thermal motions in bacteriorhodopsin at different hydration levels studied by neutron scattering: correlation with kinetics and light-induced conformational changes. Biophys J 75:1945–1952

Longeville S, Doster W, Kali G (2003) Myoglobin in crowded solutions: structure and diffusion. Chem Phys 292:413–424

Madern D (2000) The putative L-lactate dehydrogenase from *methanococcus jannaschii* is an NADPH-dependent L-malate dehydrogenase (in process citation). Mol Microbiol 37:1515–1520

Madern D (2002) Molecular evolution within the L-malate and L-lactate dehydrogenase super-family. J Mol Evol 54:825–840

Moreno JM, Sinisterra JV (1994) Immobilization of lipase from *Candida cylindracea* on inorganic supports. J Mol Catal 93:357–369

Réat V, Zaccai G, Ferrand M, Pfister C (1997) Biological macromolecular dynamics. Adenine Press, Schenectady, NY, USA

Riveros-Moreno V, Wittenberg JB (1972) The self-diffusion coefficients of myoglobin and hemoglobin in concentrated solutions. J Biol Chem 247:895–901

Simpson HD, Haufler UR, Daniel RM (1991) An extremely thermostable xylanase from the thermophilic eubacterium Thermotoga. Biochem J 277(Pt 2):413–417

Sinisterra JV (1997) Immobilization of enzymes on inorganic supports by covalent methods. In: Bickerstaff GF (ed) Immobilization of enzymes and cells. Humana Press, Totowa

Smith JC (1991) Protein dynamics: comparison of simulations with inelastic neutron scattering experiments. Q Rev Biophys 24:227–291

Tanaka A, Tosa T, Kobayashi T (1993) Industrial applications of immobilized biocatalysts, vol 21. Dekker, New York

Tehei M, Madern D, Pfister C, Zaccai G (2001) Fast dynamics of halophilic malate dehydrogenase and BSA measured by neutron scattering under various solvent conditions influencing protein stability. Proc Natl Acad Sci USA 98:14356–14361

Tehei M, Madern D, Franzetti B, Zaccai G (2005) Neutron scattering reveals the dynamic basis of protein adaptation to extreme temperature. J Biol Chem 280:40974–40979

Tehei M, Smith JC, Monk C, Ollivier J, Oettl M, Kurkal V, Finney JL, Daniel RM (2006) Dynamics of immobilized and native *Escherichia coli* dihydrofolate reductase by quasielastic neutron scattering. Biophys J 90:1090–1097

Volino F, Dianoux AJ (1980) Neutron incoherent scattering law for diffusion in a potential of spherical symmetry: general formalism and application to diffusion inside a sphere. Mol Phys 41:271–279

Zaccai G (2000) How soft is a protein? A protein dynamics force constant measured by neutron scattering. Science 288:1604–1607

Zhou HX, Dill KA (2001) Stabilization of proteins in confined spaces. Biochemistry 40:11289–11293